Calculation of electronic and magnetic properties of CuO$_2$ sheets using a modified mean-field approximation

V. F. Elesin, L. A. Openov, and E. G. Kholmovskiĭ

Moscow State Engineering Physics Institute, 115409 Moscow, Russia

A new method is proposed for calculating the electronic and magnetic properties of a CuO$_2$ sheet (the general structural element of the copper-oxide high-temperature superconductors) in the framework of the Emery model. This method is a modified mean-field approximation that takes into account adequately the antiferromagnetic correlations of the copper spins. Detailed investigations are made of the distribution of the carriers between the copper and oxygen sites, the density of states and its change on doping, the dependence of the Fermi energy on the type of doping and the carrier concentration, and the dependence of the sublattice magnetization and of the magnetic form factor on the level of p-type and n-type doping. The obtained results agree with modern ideas about the undoped precursors of high-T_c superconductors as charge-transfer insulators and correctly describe the basic way in which the insulating state is changed by doping, including the different occupancies of the copper and oxygen orbitals in the case of p-type and n-type doping, the pinning of the Fermi level, the transfer of the spectral weight, and the more rapid suppression of the antiferromagnetic correlations in the case of p-type doping than with n-type doping. The spectrum of Fermi quasiparticles is found explicitly, and the dependence of the width of the lower Hubbard band on the carrier concentration is obtained. The results for finite Cu–O clusters agree to high accuracy with numerical calculations made by exact diagonalization and by the Monte Carlo method. © *1996 American Institute of Physics.* [S1063-7761(96)01802-4]

1. INTRODUCTION

It follows from band-structure calculations[1,2] and x-ray and optical spectroscopy experiments[3,4] that the properties of high-T_c superconductors are largely determined by the interaction of the electrons of the outer shells of copper and oxygen in CuO$_2$ sheets, which are the common structural elements of copper-oxide high-T_c superconductors. The maximum overlap integral is obtained for the Cu$3d_{x^2-y^2}$ and O$2p_{x(y)}$ orbitals, which form the spectrum of electron states in the neighborhood of the Fermi level.[5] In consequence of this fact and also the presence in high-T_c superconductors of strong Coulomb correlations, the two-dimensional many-band model of Emery[6] is usually used to describe the electronic structure of the CuO$_2$ sheets.

In the analysis of the Emery model, the main difficulty is that the energy U_d of the Coulomb repulsion of the carriers at the copper sites is too large to include the Coulomb correlations in perturbation theory [U_d=6–10 eV (Refs. 5 and 7), which is of the order of the band width] but too small for correct expansion with respect to the parameter t/U_d (Refs. 8 and 9), where $t≈1$ eV is the matrix element of a carrier hop along the copper–oxygen bonds. Since the difference ε of the carrier energies at the oxygen and copper sites has the order of magnitude t (Refs. 5 and 7), expansion with respect to the parameter t/ε (Refs. 9 and 10) is also invalid.

The absence of exact solutions of the Emery model stimulated development of numerical methods for modeling the electronic structure of two-dimensional Cu–O clusters— the elementary units of a CuO$_2$ sheet. The method of exact diagonalization[11–13] and the Monte Carlo method[13–16] are

most frequently used. A serious shortcoming of these methods is the severe restriction on the size of the investigated system (10–20 atoms in the first case and 20–200 atoms in the second). In addition, the accuracy of the Monte Carlo algorithm falls sharply when the temperature is lowered, so that it is not possible to investigate the most interesting case $T≤T_c≈100$ K.

To describe the electronic structure of an infinite CuO$_2$ sheet, different (analytic or semianalytic) approaches are used. The difficulty is that in the undoped (insulating) and weakly doped (superconducting) states, which have the greatest interest, antiferromagnetic interactions, which cannot be described by the means of the standard mean-field approximation, are very strong. This approximation is not capable of explaining the antiferromagnetic insulating state of the undoped system and the insulator–metal phase transition resulting from doping. The assumption of a paramagnetic state of the CuO$_2$ sheet[17,18] leads to a discrepancy with the data of cluster calculations.[15]

To take into account antiferromagnetic correlations of the copper spins due to the large value of U_d, one most often uses the slave-boson method, which was proposed in Ref. 19 for the single-band Hubbard model and generalized in Refs. 20 and 21 to the many-band Emery model. Other approaches are known (see, for example, Ref. 22), but they are less popular. To some degree or other, all these methods are approximate, and therefore it is sometimes difficult to know how well they describe the properties of a real system. One of the possible criteria here could be the agreement between analytic results and the data of exact numerical calculations of finite Cu–O clusters. As examples, we may mention the

good agreement between the properties of the ground state of the Cu_4O_8 cluster as calculated by the slave-boson method and the method of exact diagonalization,[23] and also the similarity of the phase diagrams describing the bound states of the excess holes in a CuO_2 sheet[22,24] and the Cu_4O_8 cluster[25] with infinitely large U_d.

Every approximate method has certain shortcomings. For example, the algorithm developed for the Emery model in Ref. 22 can be used only in the limiting case $t \ll \varepsilon$, which does not correspond to the real experimental situation $t \approx \varepsilon$ (Refs. 5 and 7) and restricts its applicability. A serious shortcoming of the slave-boson method is that the quasiparticles in it are composite Fermi–Bose formations. This makes it necessary to take into account several subsidiary conditions (constraints[19]) and makes it difficult to calculate the properties of the actual Fermi quasiparticles (for example, their dispersion[21]). In addition, because of the comparatively large number of variational parameters it is necessary to use rather laborious numerical calculations to obtain actual results by the slave-boson method.

In this paper, we propose a new method for calculating the electronic and magnetic properties of a CuO_2 sheet. Although it is based on the mean-field approximation, it does take into account explicitly the presence of antiferromagnetic correlations in both the undoped and doped states. In contrast with Ref. 22, this method can be used for an arbitrary relationship between the parameters of the Emery model, and, in contrast with the slave-boson method, makes it possible to find explicitly the dispersion and wave functions of the actual Fermi quasiparticles, and not "pseudofermions"; this greatly facilitates its application to the calculation of the electronic and magnetic properties of the CuO_2 sheets, namely, the occupancies of the atomic orbitals, the spectrum of the Fermi quasiparticles, the band width, the density of states, the antiferromagnetic correlations, etc. At the same time, it is possible to obtain an effectively complete analytic solution (numerical calculations are required only in the self-consistency stage, and the number of variational parameters is less than in the slave-boson method, which greatly accelerates the convergence and shortens the time of the numerical calculations by 1–2 orders of magnitude). The method can also be applied to finite Cu–O clusters; the results that are then obtained agree excellently with the data of the exact diagonalization and Monte Carlo methods. Good agreement with the experimental data indicates that the method correctly describes the main features of the electronic structure of high-T_c superconductors.

2. METHOD OF CALCULATION

The starting point of our method is the two-dimensional many-band model of Emery,[6] the Hamiltonian of which has the form

$$H = -t \sum_{\langle ij \rangle, \sigma} (d_{i\sigma}^+ p_{j\sigma} + \text{h.c.}) + \varepsilon_d \sum_{i,\sigma} n_{i\sigma} + \varepsilon_p \sum_{j,\sigma} n_{j\sigma}$$
$$+ U_d \sum_i n_{i\uparrow} n_{i\downarrow} + V \sum_{\langle ij \rangle, \sigma, \sigma'} n_{i\sigma} n_{j\sigma'} + U_p \sum_j n_{j\uparrow} n_{j\downarrow},$$
(1)

where $d_{i\sigma}^+$ and $p_{j\sigma}^+$ are the operators of creation of a hole in the states $3d_{x^2-y^2}$ and $2p_{x(y)}$, respectively, $\langle ij \rangle$ denotes summation over nearest neighbors, the index i labels the copper sites and the index j the oxygen sites, $n_{i\sigma} = d_{i\sigma}^+ d_{i\sigma}$, $n_{j\sigma} = p_{j\sigma}^+ p_{j\sigma}$, t is the matrix element of a copper–oxygen hop, $\varepsilon_p (\varepsilon_d)$ are the hole energies at the oxygen (respectively, copper) sites, and U_d, U_p, and V are the energies of the Coulomb repulsion of holes at the copper and oxygen sites and between them, respectively.

In the undoped insulating state of the high-T_c superconductor, there is one hole at each copper atom in the CuO_2 sheet, i.e., there is one hole for each CuO_2 unit cell, and therefore it is convenient to use the hole representation of the Hamiltonian (1). An increase in the number of holes in the CuO_2 sheet corresponds to p-type doping of the high-T_c superconductor (partial replacement of La^{3+} by Sr^{2+} in La_2CuO_4, lowering of the oxygen deficit δ in $YBa_2Cu_3O_{7-\delta}$, etc.) while a decrease of the number corresponds to n-type doping (partial replacement of Nd^{3+} by Ce^{4+} in Nd_2CuO_4 or of Sr^{2+} by La^{3+} in $SrCuO_2$, etc.).

Our aim is to transform the Hamiltonian (1) to a single-particle form in order to take into account the possible presence at the copper sites of antiferromagnetic spin correlations, which occur at a low doping level of the CuO_2 sheets. Since these correlations are due to the strong Coulomb repulsion of the holes at the copper sites ($U_d \gg t$), in the first stage we apply the Hartree–Fock decoupling only to the last two terms in (1), which describe the interaction of holes at the copper sites and at neighboring copper and oxygen sites. Proceeding in this manner, we assume that these interactions do not have a decisive effect on the electronic structure of the CuO_2 sheet, i.e., that they lead to quantitative but not qualitative changes in the spectrum. This is true if U_p and V are much less than U_d, which certainly appears to be the case in high-T_c superconductors (see, for example, Ref. 5). With allowance for what we have said above, we obtain

$$V \sum_{\langle ij \rangle, \sigma, \sigma'} n_{i\sigma} n_{j\sigma'} \approx 4V n_p \sum_{i,\sigma} n_{i\sigma} + 2V n_d \sum_{j,\sigma} n_{j\sigma}$$
$$- V n_{pd} \sum_{\langle ij \rangle, \sigma} (d_{i\sigma}^+ p_{j\sigma} + \text{h.c.})$$
$$- 4N V n_d n_p + 8N V n_{pd}^2,$$
(2)

$$U_p \sum_j n_{j\uparrow} n_{j\downarrow} \approx U_p (n_p/2) \sum_{j,\sigma} n_{j\sigma} - (N/2) U_p n_p^2,$$
(3)

where $n_p = \langle n_{j\uparrow} \rangle + \langle n_{j\downarrow} \rangle$ and $n_d = \langle n_{i\uparrow} \rangle + \langle n_{i\downarrow} \rangle$ are the occupancies of the oxygen and copper sites, respectively, $n_{pd} = \langle d_{i\sigma}^+ p_{j\sigma} \rangle = \langle p_{j\sigma}^+ d_{i\sigma} \rangle_h$, $\langle ... \rangle$ denotes the mean value in the ground state (at $T=0$) or over the canonical ensemble (at finite temperature), and N is the number of CuO_2 cells in the

system. In (2), allowance is made for the fact that the nearest neighbors of each copper atom are four oxygen atoms, while the nearest neighbors of each oxygen atom are two copper atoms. With allowance for (2) and (3), the Hamiltonian (1) takes the form

$$H = -t' \sum_{\langle ij \rangle, \sigma} (d_{i\sigma}^+ p_{j\sigma} + \text{h.c.}) + \varepsilon_d' \sum_{i,\sigma} n_{i\sigma} + \varepsilon_p' \sum_{j,\sigma} n_{j\sigma}$$

$$+ U_d \sum_i n_{i\uparrow} n_{i\downarrow} + E', \qquad (4)$$

where

$$t' = t + V n_{pd}, \quad \varepsilon_d' = \varepsilon_d + 4 V n_p, \quad \varepsilon_p' = \varepsilon_p + 2 V n_d$$

$$+ (U_p/2) n_p,$$

$$E' = 8 N V n_{pd}^2 - 4 N V n_d n_p - (N/2) U_p n_p^2.$$

If the mean field approximation can also be applied to the term that characterizes the repulsion of the holes at the copper sites, then one can describe fairly well the paramagnetic phase of the CuO_2 sheet,[18] which corresponds to a heavily doped nonsuperconducting state. However, one does not then take into account the antiferromagnetic correlations, which have a decisive effect on the electrical and magnetic properties of the undoped insulating state[26-29] and, possibly, play a decisive role in the formation of the superconducting state in the case of a weak doping level.[30]

In order to take into account the antiferromagnetic correlations adequately, we divide the copper lattice into two sublattices in the coordinate and spin space, and then use the mean field approximation. Such an approach enables us to find the dispersion law of the actual Fermi quasiparticles in an antiferromagnetic environment without having to introduce Fermi–Bose quasiparticles as in the slave-boson method. At the same time, the physical picture becomes completely transparent, and the calculation of the various electronic and magnetic properties is significantly simplified. In addition, we shall see that our approach admits an almost complete analytic solution (laborious numerical calculations are required only in the final stage of obtaining self-consistency).

Mathematically, our approach can be formulated as follows. We make the ansatz

$$d_{i\sigma}^A = d_{i\sigma}[1 + \sigma \exp(i \mathbf{Q} \cdot \mathbf{R}_i)]/2,$$

$$d_{i\sigma}^B = d_{i\sigma}[1 - \sigma \exp(i \mathbf{Q} \cdot \mathbf{R}_i)]/2, \qquad (5)$$

where $\mathbf{R}_i$ are the coordinates of the copper sites, $\mathbf{Q} = (\pi/a, \pi/a)$, a is the distance between the nearest-neighbor copper sites (the lattice period), and $\sigma = +1$ and -1 (for spin directions upward and downward, respectively). Some properties of the operators $d_{i\sigma}^A$ and $d_{i\sigma}^B$ and also their connection with the operators $d_{i\sigma}$ and $n_{i\sigma}$ are given in Appendix 1. By means of the ansatz (5), we have divided the copper lattice of the CuO_2 sheet into two sublattices (A and B) in coordinate–spin space. The sites of the A and B sublattices coincide in coordinate space but differ in spin space (Fig. 1). Each site of an A or B sublattice can be occupied only once, i.e., by a hole with spin up or a hole with spin down, depending on the
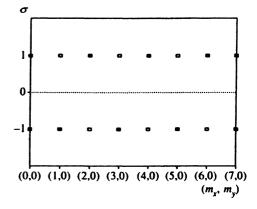

FIG. 1. Division of the copper lattice into the coordinate–spin space. The coordinates of the copper sites are $\mathbf{R} = a m_x \mathbf{e}_x + a m_y \mathbf{e}_y$ (a is the lattice period). As an example, one of the directions in the CuO_2 plane is shown. The solid and open squares show the A and B sublattices, respectively.

coordinate of the site. For example, the site of the A sublattice with spatial coordinates $\mathbf{R}_i = (0;0)$ can be occupied only by a hole with spin up, while the site of the B sublattice with the same spatial coordinates can be occupied only by a hole with spin down.

The term with U_d in (4) now takes the form

$$H_{U_d} = U_d \sum_i (n_{i\uparrow}^A n_{i\downarrow}^B + n_{i\downarrow}^A n_{i\uparrow}^B), \qquad (6)$$

where $n_{i\sigma}^A = d_{i\sigma}^{A+} d_{i\sigma}^A$, $n_{i\sigma}^B = d_{i\sigma}^{B+} d_{i\sigma}^B$. The use of the mean field approximation at this stage makes it possible to describe the antiferromagnetic ordering of the copper spins if there is such ordering in the system. Applying the Hartree–Fock decoupling, we obtain from (6)

$$H_{U_d} \approx U_d \sum_i (\langle n_{i\uparrow}^A \rangle n_{i\downarrow}^B + n_{i\uparrow}^A \langle n_{i\downarrow}^B \rangle - \langle n_{i\uparrow}^A \rangle \langle n_{i\downarrow}^B \rangle)$$

$$+ U_d \sum_i (\langle n_{i\uparrow}^B \rangle n_{i\downarrow}^A + n_{i\uparrow}^B \langle n_{i\downarrow}^A \rangle - \langle n_{i\uparrow}^B \rangle \langle n_{i\downarrow}^A \rangle). \qquad (7)$$

Note that for each copper site i only one of the mean values $\langle n_{i\uparrow}^A \rangle$ or $\langle n_{i\downarrow}^A \rangle$ is nonzero (the same is also true for $\langle n_{i\uparrow}^B \rangle$, $\langle n_{i\downarrow}^B \rangle$). We shall assume that the numbers of carriers with spin up and spin down are the same. Then, depending on the site number i, we obtain $\langle n_{i\uparrow}^A \rangle \equiv n^A$, $\langle n_{i\downarrow}^A \rangle = 0$ or $\langle n_{i\downarrow}^A \rangle \equiv n^A$, $\langle n_{i\uparrow}^A \rangle = 0$. For the B sublattice, we have $\langle n_{i\uparrow}^B \rangle \equiv n^B$, $\langle n_{i\downarrow}^B \rangle = 0$ or $\langle n_{i\downarrow}^B \rangle \equiv n^B$, $\langle n_{i\uparrow}^B \rangle = 0$. Here n^A (n^B) is the probability of occupation by a hole of a site of the A (respectively, B) copper sublattice. Depending on the values of n^A and n^B, one or other of the following phases will be realized in the system: 1) for $n^A = n^B$, the paramagnetic phase, i.e., any copper site will be occupied with equal probability by carriers having opposite spin directions; 2) for $n^A \neq n^B$, the antiferromagnetic phase, i.e., the A and B sublattices are occupied by carriers with different probabilities.

It is here necessary to make the following remark. Since the A and B sublattices are completely equivalent, in the absence of a magnetic field the antiferromagnetic states with $n^A > n^B$ and $n^B > n^A$ do not differ in any way, since the one can be obtained from the other by the substitution $A \leftrightarrow B$. Therefore, the state of the system is doubly degenerate. In

reality, however, the transition from the phase with $n^A = n^B$ to the phase with $n^A \neq n^B$ spontaneously lifts of the degeneracy (an analogous situation obtains, for example, in the Ising model). In other words, the situation is as if there were an infinitesimal magnetic field present in the system. In what follows, we shall for definiteness assume that $n^A \geqslant n^B$.

Using the notation n^A and n^B, we write (7) in the form

$$H_{U_d} = U_d n^A \sum_{i,\sigma} n_{i\sigma}^B + U_d n^B \sum_{i,\sigma} n_{i\sigma}^A - NU_d n^A n^B. \qquad (8)$$

Substituting (8) in (4) and making the change of variables (5), we obtain

$$H = -t' \sum_{\langle ij \rangle, \sigma} ((d_{i\sigma}^{A+} + d_{i\sigma}^{B+}) p_{j\sigma} + \text{h.c.}) + \varepsilon_d^A \sum_{i,\sigma} n_{i\sigma}^A$$

$$+ \varepsilon_d^B \sum_{i,\sigma} n_{i\sigma}^B + \varepsilon_p' \sum_{j,\sigma} n_{j\sigma} + E'', \qquad (9)$$

where

$$\varepsilon_d^A = \varepsilon_d' + U_d n^B, \quad \varepsilon_d^B = \varepsilon_d' + U_d n^A,$$

$$E'' = E' - NU_d n^A n^B;$$

the expressions for ε_d', ε_p', t', and E' are given above.

The Hamiltonian (9) is a single-particle Hamiltonian, and it can therefore be diagonalized by going to the $\mathbf{k}$ representation. However, it is convenient as a preparation, using an ansatz similar to (5), to divide the copper lattice of the CuO_2 plane into sublattices A and B:

$$p_{i\sigma}^{1A} = p_{i\sigma}^1 [1 + \sigma \exp(i\mathbf{Q} \cdot \mathbf{R}_i)]/2,$$

$$p_{i\sigma}^{1B} = p_{i\sigma}^1 [1 - \sigma \exp(i\mathbf{Q} \cdot \mathbf{R}_i)]/2,$$

$$p_{i\sigma}^{2A} = p_{i\sigma}^2 [1 + \sigma \exp(i\mathbf{Q} \cdot \mathbf{R}_i)]/2,$$

$$p_{i\sigma}^{2B} = p_{i\sigma}^2 [1 - \sigma \exp(i\mathbf{Q} \cdot \mathbf{R}_i)]/2,$$

where $p_{i\sigma}^1 (p_{i\sigma}^2)$ are the operators for annihilation of a hole in the states $2p_x(2p_y)$ at the copper sites with coordinates $\mathbf{R}_i + \mathbf{e}_x a/2 (\mathbf{R}_i + \mathbf{e}_y a/2)$. Here $\mathbf{R}_i = \mathbf{e}_x m_x a + \mathbf{e}_y m_y a$ are the coordinates of the copper sites (m_x and m_y are integers). We emphasize that the transition to the new p operators is made exclusively for reasons of convenience in subsequent manipulations and does not signify (as in the case of the copper sublattice) the presence of antiferromagnetic correlations of the spins at the oxygen sites.

The Hamiltonian (9) can now be expressed completely in terms of variables relating to the A and B copper and oxygen sublattices: $H = H_0 + H_t$, where the diagonal part has the form

$$H_0 = \varepsilon_d^A \sum_{i,\sigma} d_{i\sigma}^{A+} d_{i\sigma}^A + \varepsilon_d^B \sum_{i,\sigma} d_{i\sigma}^{B+} d_{i\sigma}^B + \varepsilon_p' \sum_{i,\sigma} (p_{i\sigma}^{1A+} p_{i\sigma}^{1A}$$

$$+ p_{i\sigma}^{1B+} p_{i\sigma}^{1B} + p_{i\sigma}^{2A+} p_{i\sigma}^{2A} + p_{i\sigma}^{2B+} p_{i\sigma}^{2B}) + E'',$$

and the hops are described by the term

$$H_t = -t' \sum_{m_x, m_y, \sigma} \{d_{m_x, m_y, \sigma}^{A+} (p_{m_x, m_y, \sigma}^{1A} + p_{m_x, m_y, \sigma}^{2A}$$

$$+ p_{m_x - 1, m_y, \sigma}^{1B} + p_{m_x, m_y - 1, \sigma}^{2B}) + d_{m_x, m_y, \sigma}^{B+} (p_{m_x, m_y, \sigma}^{1B}$$

$$+ p_{m_x, m_y, \sigma}^{2B} + p_{m_x - 1, m_y, \sigma}^{1A} + p_{m_x, m_y - 1, \sigma}^{2A}) + \text{h.c.}\}: \qquad (10)$$

where $d_{m_x, m_y, \sigma}^{A+}$, $p_{m_x, m_y, \sigma}^{1A+}$ and $p_{m_x, m_y, \sigma}^{2A+}$ are the operators for creation of a hole in the states $3d_{x^2-y^2}$, $2p_x$, and $2p_y$, respectively, for the states of the unit cell that belong to the copper and oxygen A sublattices. The operators with index B are the ones for the corresponding B sublattices.

The Hamiltonian (10) can be diagonalized in the usual manner. The single-particle wave function of a hole with quasimomentum $\mathbf{k} = (k_x, k_y)$ and spin projection σ has the general form

$$\Psi_{\mathbf{k}, \sigma}(\mathbf{r}) = C_A(\mathbf{k})\Psi_{\mathbf{k}\sigma}^A(\mathbf{r}) + C_B(\mathbf{k})\Psi_{\mathbf{k}\sigma}^B(\mathbf{r})$$

$$+ C_{1A}(\mathbf{k})\Psi_{\mathbf{k}\sigma}^{1A}(\mathbf{r}) + C_{1B}(\mathbf{k})\Psi_{\mathbf{k}\sigma}^{1B}(\mathbf{r})$$

$$+ C_{2A}(\mathbf{k})\Psi_{\mathbf{k}\sigma}^{2A}(\mathbf{r}) + C_{2B}(\mathbf{k})\Psi_{\mathbf{k}\sigma}^{2B}(\mathbf{r}), \qquad (11)$$

where $\Psi_{\mathbf{k}\sigma}^A, \Psi_{\mathbf{k}\sigma}^B, \Psi_{\mathbf{k}\sigma}^{1A}, \Psi_{\mathbf{k}\sigma}^{1B}, \Psi_{\mathbf{k}\sigma}^{2A}, \Psi_{\mathbf{k}\sigma}^{2B}$ are Bloch wave functions constructed using the Wannier functions of the corresponding copper and oxygen sublattices. The coefficients $C_A(\mathbf{k})$ and $C_B(\mathbf{k})$ are the probabilities for finding a hole with quasimomentum $\mathbf{k}$ in the A and B copper sublattices, respectively, and $C_{1A}(\mathbf{k})$ and $C_{2A}(\mathbf{k})$ [$C_{1B}(\mathbf{k})$ and $C_{2B}(\mathbf{k})$] are the corresponding quantities for the $A(B)$ oxygen sublattices, respectively, with site coordinates $\mathbf{R}_i + \mathbf{e}_x a/2$ and $\mathbf{R}_i + \mathbf{e}_y a/2$. The normalization condition is

$$|C_A(\mathbf{k})|^2 + |C_B(\mathbf{k})|^2 + |C_{1A}(\mathbf{k})|^2 + |C_{1B}(\mathbf{k})|^2$$

$$+ |C_{2A}(\mathbf{k})|^2 + |C_{2B}(\mathbf{k})|^2 = 1.$$

Substituting (11) in the Schrödinger equation

$$H\Psi_{\mathbf{k}\sigma}(\mathbf{r}) = E(\mathbf{k})\Psi_{\mathbf{k}\sigma}(\mathbf{r}),$$

where the Hamiltonian H has the form (10), we obtain a system of equations for the coefficients $C_A, C_B, C_{1A}, C_{1B}, C_{2A}, C_{2B}$ (see Appendix 2). The condition for the existence of a nontrivial solution of this system gives the dispersion law $E_l(\mathbf{k})$, where $l = 1-6$ is the band index. For $l = 1$ and 2, we have $E_1(\mathbf{k}) = E_2(\mathbf{k}) = \varepsilon_p'$. We find the values of $E_3(\mathbf{k}), E_4(\mathbf{k}), E_5(\mathbf{k})$, and $E_6(\mathbf{k})$ by solving the equation

$$(\varepsilon_d^A - E)(\varepsilon_d^B - E)(\varepsilon_p' - E)^2 - 4t'^2(\varepsilon_p' - E)(\varepsilon_d^A + \varepsilon_d^B$$

$$- 2E) + 4t'^4 S(\mathbf{k}) = 0, \qquad (12)$$

where

$$S(\mathbf{k}) = 4 - [\cos(k_x a) + \cos(k_y a)]^2.$$

Explicit expressions for $E_3(\mathbf{k})$, $E_4(\mathbf{k})$, $E_5(\mathbf{k})$, and $E_6(\mathbf{k})$ are given in Appendix 3.

In the k representation, the Hamiltonian (10) is diagonal:

$$H = \sum_{l=1}^{6} \sum_{\mathbf{k}, \sigma}{}' E_l(\mathbf{k}) Z_{\mathbf{k}, \sigma}^{l+} Z_{\mathbf{k}, \sigma}^l, \qquad (13)$$

where

$$Z^l_{\mathbf{k},\sigma} = C^l_A(\mathbf{k})d^A_{\mathbf{k},\sigma} + C^l_B(\mathbf{k})d^B_{\mathbf{k},\sigma} + C^l_{1A}(\mathbf{k})p^{1A}_{\mathbf{k},\sigma}$$

$$+ C^l_{1B}(\mathbf{k})p^{1B}_{\mathbf{k},\sigma} + C^l_{2A}(\mathbf{k})p^{2A}_{\mathbf{k},\sigma} + C^l_{2B}(\mathbf{k})p^{2B}_{\mathbf{k},\sigma}.$$

The prime in (13) means that the summation is over half the Brillouin zone. The region of summation in the **k** space decreases because the lattice period in real space doubles after the division into the A and B sublattices.

For $l = 1$ and 2, we have $|C^l_A(\mathbf{k})|^2 = |C^l_B(\mathbf{k})|^2 = 0$, i.e., the first and second bands are occupied exclusively by carriers in the $2p$ oxygen orbitals; moreover, the probabilities of occupation of the A and B oxygen sublattices are equal. These are so-called nonbonding bands corresponding to the atomic level of $2p$ oxygen orbitals. They are nondispersive because we have ignored direct oxygen–oxygen hops in the original Hamiltonian (1). The remaining bands are occupied by both holes in the $3d_{x^2-y^2}$ orbitals and holes in the $2p_{x(y)}$ orbitals. The values of $|C^l_A|^2$, $|C^l_B|^2$, $|C^l_{1A}|^2$, $|C^l_{1B}|^2$, $|C^l_{2A}|^2$, $|C^l_{2B}|^2$ are given in Appendix 4. Note that the probabilities of occupation of the $2p_x$ and $2p_y$ orbitals of the different sublattices are the same for all bands: $|C^l_{1A}(\mathbf{k})|^2 = |C^l_{1B}(\mathbf{k})|^2$ and $|C^l_{2A}(\mathbf{k})|^2 = |C^l_{2B}(\mathbf{k})|^2$.

There are two possible cases corresponding to different types of occupancy of the A and B copper sublattices: 1) the paramagnetic phase ($U_d = 0$, $n^A = n^B$), for which the probabilities of occupation of all the bands by carriers in the $3d_{x^2-y^2}$ orbitals of the A and B copper sublattices are equal ($|C^l_A(\mathbf{k})|^2 = |C^l_B(\mathbf{k})|^2$, see Appendix 4); 2) the antiferromagnetic phase ($U_d > 0$, $n^A \neq n^B$), in which case $|C^l_A(\mathbf{k})|^2 \neq |C^l_B(\mathbf{k})|^2$, i.e., the probabilities of occupation of the A and B copper sublattices are different.

Now, knowing the explicit expressions for $E_l(\mathbf{k})$ and the band occupation probabilities, we write down the self-consistency conditions

$$n^A = (2/N) \sum_{l=1}^{6} {\sum_{\mathbf{k}}}' |C^l_A(\mathbf{k})|^2 f\langle E_l(\mathbf{k})\rangle, \qquad (14)$$

$$n^B = (2/N) \sum_{l=1}^{6} {\sum_{\mathbf{k}}}' |C^l_B(\mathbf{k})|^2 f(E_l(\mathbf{k})), \qquad (15)$$

$$n_{pd} = (1/N) \sum_{l=1}^{6} {\sum_{\mathbf{k}}}' [C^{l*}_A(\mathbf{k}) C^l_{1A}(\mathbf{k}) \exp(ik_x a/2)$$

$$+ C^{l*}_B(\mathbf{k}) C^l_{1B}(\mathbf{k}) \exp(ik_y a/2)] f(E_l(\mathbf{k})), \qquad (16)$$

$$n = 2n_p + n_d = 2n_p + n^A + n^B, \qquad (17)$$

where $f(E)$ is the Fermi distribution function, and n is the reduced concentration of holes (the number of holes per CuO_2 cell).

Self-consistent values of n^A, n^B, and n_{pd} were determined numerically by successive iteration. We first specified the parameters of the Emery Hamiltonian ($\varepsilon_p, \varepsilon_d, U_d, U_p, V, t$), the number of CuO_2 cells in the investigated system (N), the hole concentration (n), the temperature (T), and also the initial values of n^A, n^B, n_{pd}. We then calculated the energies $E_l(\mathbf{k})$, the band occupation probabilities $|C^l(\mathbf{k})|^2$, and the value of the chemical potential. Using the expressions (14)–(17), we determined new values of n^A, n^B, n_{pd}. If they differed from the initial values, the itera-

tive procedure was repeated with the original values of n^A, n^B, n_{pd} taken to be those obtained in the previous iteration. Such iterations were continued until the difference between the "input" and "output" values became less than a prescribed quantity, which we usually set equal to 10^{-5}.

As our calculations showed, the final result does not depend on the choice of the initial values of n^A, n^B, n_{pd}, i.e., the iterative algorithm described in this paper is stable. The number of iterations needed to achieve the accuracy 10^{-5} depends, in general, on the values of the parameters of the Emery Hamiltonian, the size of the system, the hole concentration, and also on the quality (i.e., the proximity to the true values) of the initial values of n^A, n^B, n_{pd} but, as a rule, does not exceed 50 and only in individual cases amounts to 200 or more iterations. Note that n^A, n^B, n_{pd} play qualitatively the same role as the variational coefficients λ_i in the slave-boson method.[19-21] However, there are fewer of them than there are coefficients λ_i, and this reduces the time of the numerical calculations in the iterations by 1–2 orders of magnitude.

In the determination of the properties of finite Cu–O clusters, the summation in (14)–(16) was performed over discrete values of the quasimomentum: $\mathbf{k} = (k_x, k_y) = (2\pi n_x / N_x a, 2\pi n_y / N_y a)$, where $n_x = 0, 1, ..., N_x - 1$; $n_y = 0, 1..., N_y - 1$; $N_x = N_y = \sqrt{N}$. In the case of an infinite CuO_2 sheet, the summation was replaced by integration over k_x and k_y.

3. OCCUPATION OF THE COPPER AND OXYGEN ORBITALS IN THE CASE OF p-TYPE AND n-TYPE DOPING

The question of which orbitals are occupied by the excess carriers introduced into the original insulating state as a result of doping is very important for the choice of a theoretical model capable of describing adequately the electronic structure of a high-T_c superconductor. At the present time, it has been established experimentally[31-33] that the excess holes occupy preferentially the oxygen $2p_{x(y)}$ orbitals, and excess electrons preferentially copper $3d_{x^2-y^2}$ orbitals. This is, in fact, the justification for using the many-band Emery model (and not the single-band Hubbard and $t-J$ models) in order to describe the electronic structure of the CuO_2 sheets.

However, the nature of the occupation of the copper and oxygen orbitals on doping depends strongly on the values of the parameters of the Hamiltonian (1). As is shown in Ref. 8, the type of the initial insulating state of the CuO_2 sheets at small values of U_p is basically determined by the value of $(\varepsilon + 2V)/U_d$ and belongs either to the class of Mott–Hubbard insulators (for $U_d < \varepsilon + 2V$) or to the class of charge-transfer insulators (for $U_d > \varepsilon + 2V$). In the first case, both p- and n-type doping lead to a significant change in the occupancies n_d of the copper orbitals but hardly influence the occupancies n_p of the oxygen orbitals (recall that we use the hole representation, i.e., n_d and n_p are the occupancies of the corresponding orbitals by holes; the occupancies of these orbitals by electrons are $2 - n_d$ and $2 - n_p$, respectively). In the second case, n_p increases on p-type doping faster than n_d, while n_d decreases faster than n_p in the case of n-type doping. This corresponds to the experimental situation for high-T_c superconductors, indicating that the original un-
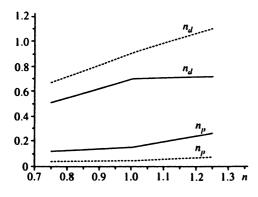
FIG. 2. Occupancies of the copper (n_d) and oxygen (n_p) orbitals versus the reduced hole concentration n for $U_d/t=6$, $\varepsilon/t=2$, $U_p=V=0$ (solid lines) and $U_d/t=2$, $\varepsilon/t=6$, $U_p=V=0$ (dashed lines). The number of CuO_2 cells in the system is $N=256$.

doped compounds La_2CuO_4, $YBa_2Cu_3O_6$, Nd_2CuO_4, $SrCuO_2$, etc. belong to the class of charge-transfer insulators.

Figure 2 gives the dependences of n_d and n_p on the number of holes n per CuO_2 unit cell ($n=1$ corresponds to the undoped insulating state, $n>1$ to p-type doping, and $n<1$ to n-type doping). The values of the parameters of the Emery model are chosen so that the initial insulating state belongs either to the class of charge-transfer insulators or to the class of Mott–Hubbard insulators. It can be seen that the nature of the dependence of n_d and n_p on n in these two cases is indeed different and identical to what was described above.

Note that the $n_p(n)$ and $n_d(n)$ curves in Fig. 2 are calculated for a Cu–O cluster consisting of $N=256$ of the CuO_2 cells. We investigated in detail the influence of the cluster size on the values of n_d and n_p. The corresponding graphs are shown in Fig. 3. It can be seen that the values of n_d and, therefore, n_p (for $n=$const) virtually cease to depend on N already at $N=16$. Thus, the occupancies are weakly sensitive to the size of the Cu–O clusters, and this can be regarded as a justification of the use of the exact diagonalization method[12,13] and the Monte Carlo method[13–16] to calculate n_d and n_p in Cu_4O_8 and $Cu_{16}O_{32}$ clusters, respectively.

Returning to Fig. 2, we emphasize that our results agree well with both experiment[31–33] and the numerical calculations of Refs. 12, 13, 15, and 16. For example, it has been established experimentally[33] that in $Re_{2-x}M_xCuO_{4-\delta}$ (Re =Pr, Nd, Sm; M=Ce, Tb) the spectral weight of the line

corresponding to holes at copper orbitals decrease by $14\pm4\%$ if x is increased from 0 to 0.15. It follows from our calculations (see Fig. 2) that at this level of n-type doping ($n=0.85$) the value of n_d is reduced by 15%—in good agreement with the experiment and with Refs. 13, 15, and 16, in which calculations were made by the Monte Carlo method.

In order to make a more detailed comparison of our results with the data of numerical cluster calculations, we found the function $n_d(\varepsilon)$ for the Cu_4O_8 and $Cu_{16}O_{32}$ clusters and compared them with studies in which these functions were found by the exact diagonalization method[13] and the Monte Carlo method.[15] The corresponding curves are given in Fig. 4. For the Cu_4O_8 cluster, the difference between our calculated values and the exact numerical values of n is less than 3% in the complete range $\varepsilon/t=0–5$; moreover, in the most interesting region (corresponding to the real experimental situation) $\varepsilon/t=1–2$ the $n_d(\varepsilon)$ curves practically coincide (see Fig. 4a). For the $Cu_{16}O_{32}$ cluster, our values of n_d differ from those given in Ref. 15 by 1–2% (see Fig. 4).

We investigated in detail how n_d and n_p depend on U_p, U_d, V, and ε for different n. We found that a change in U_p had very little effect on n_d when $n<1$. This is because in both charge-transfer and Mott–Hubbard insulators the excess electrons preferentially occupy copper orbitals. In the Mott–Hubbard insulators, such a situation also obtains in the case of p-type doping ($n>1$). In the charge-transfer insulators, increase of U_p for $n>1$ causes n_d to grow. For $n<1$ the value of U_d also has a weak effect on the distribution of the carriers between the copper and oxygen orbitals. However, for $n>1$ the occupancies depend strongly on U_d (n_d decreases rapidly with increasing U_d). In contrast to the parameters U_p and U_d, variation of V leads not only to quantitative but also to qualitative changes of n_d and n_p. We established that increase of V to a certain critical value $V_c>\varepsilon$ causes to an abrupt redistribution of the holes between the copper and oxygen sites. At the same time, n_d decreases abruptly, and n_p, correspondingly, increases. Similar results were obtained in Ref. 34.

Summarizing this section, we note that the modified mean field approximation that we have proposed in this paper describes not only qualitatively but also quantitatively correctly the dependence of the occupancies of the copper and oxygen orbitals on the parameters of the Emery model and on the doping level. This follows both from comparison
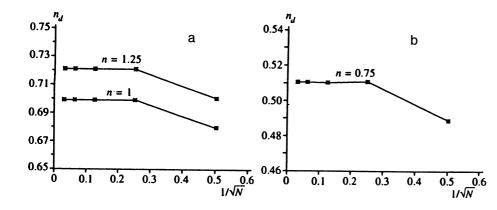

FIG. 3. Occupancies n_d of the copper orbitals versus the number N of CuO_2 cells in the Cu–O cluster for $U_d/t=2$, $\varepsilon/t=6$, $U_p=V=0$; a) undoped insulating state ($n=1$); p-type doping ($n=1.25$); b) n-type doping ($n=0.75$).
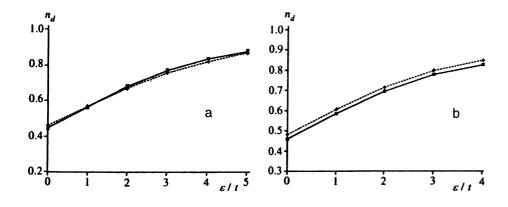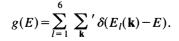
FIG. 4. Occupancies n_d of the copper orbitals versus ε for $U_d/t=6$, $U_p=V=0$, $n=1$. a) The Cu_4O_8 cluster; b) the $Cu_{16}O_{32}$ cluster; the solid lines are the results of our calculations, and the dashed lines give the data of the exact diagonalization method[13] (a) and Monte Carlo method[15] (b).

with experimental data and from the agreement with the numerical first-principles calculations made for some Cu–O clusters. Our approach also makes it possible to investigate how the occupancies depend on the size of the system. This enabled us to determine the size of the Cu–O cluster at which its properties differ weakly from those of an infinite CuO_2 sheet. This is important for an analysis of the results obtained by the numerical methods: exact diagonalization and Monte Carlo.

4. DENSITY OF STATES

The occupancies of the copper and oxygen orbitals are rather crude characteristics of the system in question. Much more informative is a quantity such as the density $g(E)$ of quasiparticle states, which is defined by

$$g(E)=\sum_{l=1}^{6}\sum_{\mathbf{k}}{}'\,\delta(E_l(\mathbf{k})-E).$$

The chemical potential μ was found from the condition

$$n=2N^{-1}\int_{-\infty}^{\infty}g(E)f(E,\mu)dE,$$

where $f(E,\mu)$ is the Fermi distribution function.

In this paper, we have restricted ourselves to investigating the influence of doping on $g(E)$ and $E_f=\mu(T=0)$. Figure 5 gives the $g(E)$ curves for a CuO_2 sheet for different doping levels [we emphasize that $g(E)$ depends strongly on the carrier concentration, i.e., the scheme of the energy bands is not "rigid"]. The form of the function $g(E)$ reflects the presence in the energy spectrum of five bands: the lower
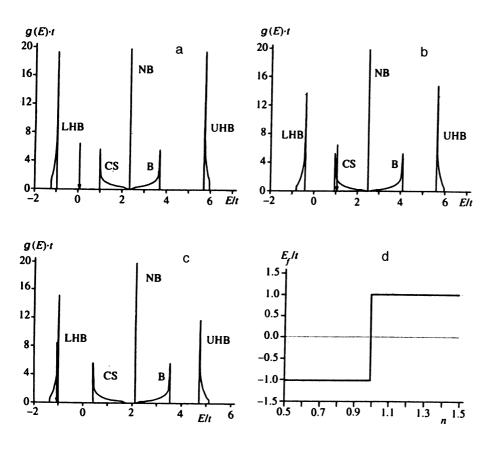

FIG. 5. Density of quasiparticle states $g(E)$ in a CuO_2 sheet for $U_d/t=6$, $\varepsilon/t=1.5$, $U_p/t=2$, $V/t=0.5$. The arrow indicates the position of the Fermi level E_f. The lower Hubbard band is LHB, the upper Hubbard band is UHB, the band of correlated states is CS, the nonbonding oxygen band is NB, and the bonding copper–oxygen band is B. a) Undoped insulating state ($n=1$); b) p-type doping ($n=1.25$); c) n-type doping ($n=0.75$); d) dependence of the Fermi energy E_f on the reduced hole concentration n.
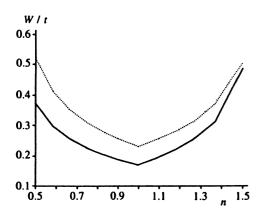
FIG. 6. Width W of the lower Hubbard band versus the reduced hole concentration n. The dashed line is for $U_d/t=6$, $\varepsilon/t=2$, $U_p=V=0$, and the solid line for $U_d/t=2$, $\varepsilon/t=6$, $U_p=V=0$.

Hubbard band (LHB), the bands of correlated states (CS), the doubly degenerate nonbonding band (NB), the bonding band (B), and the upper Hubbard band (UHB). These bands are named in accordance with the studies of Refs. 35 and 36.

The LHB and UHB are separated by $\approx U_d$. They are formed by quasiparticle states, to which the copper orbitals make the main contribution. We note that for $n=1$ it is predominantly orbitals relating to the copper A sublattice that are occupied in the LHB, and only a small fraction of carriers occupy copper orbitals of the B sublattice. For the UHB, the opposite situation is realized. Between the two Hubbard bands, there are the purely oxygen NB at $E = \varepsilon_p'$, the CS, and the bonding band.

In the case of p-type doping, the LHB is shifted to higher energies. This effect was found experimentally in an investigation of x-ray absorption in $La_{2-x}Sr_xCuO_4$ (in the case of p-type doping, the LHB spectral intensity was shifted in the direction of the band in which the Fermi level is situated[37,38]). Doping of n-type leads to a shift of the CS band to lower energies, i.e., to the region in which the band gap is situated in the undoped state. A similar shift of the spectral intensity has been observed experimentally in an n-type high T_c superconductor.[39]

It can be seen from Fig. 5 that for $n=1$ the Fermi level is situated in the band gap. For $t\approx1$ eV, the gap width is of order 2 eV, in agreement with the experimental data of Refs. 40 and 41. Weak p-type doping leads to a displacement of E_f into the CS band, after which E_f hardly changes with further doping (pinning of the Fermi level). In the case of weak n-type doping, E_f is shifted into the LHB and then depends very weakly on n, as in the case of p-type doping. Note that the qualitative dependence of E_f on n (Fig. 5d) agrees qualitatively with the experimental studies of Refs. 33, 37, 38, and 42, in which it was shown that on the transition from p- to n-type doping there is an abrupt "transfer" of E_f from one side of the band gap to the other. Admittedly, this contradicts the data of photoemission spectroscopy,[43] according to which E_f is approximately the same for both types of doping. One of the possible reasons for such a discrepancy is that the photoemission experiments give information only on the properties of a narrow surface layer of the sample.

Figure 6 gives the dependences of the LHB width W on n for different values of the model parameters. It can be seen that $W(n)$ has a minimum at $n=1$. This is due to the presence of the metal–insulator phase transition at this carrier concentration. We emphasize that for $U_d=U_p=V=0$ the band structure is "rigid," i.e., does not depend on n.

5. MAGNETIC PROPERTIES

In undoped copper-oxide insulators, there is antiferromagnetic ordering of the magnetic moments at the copper sites, and therefore these compounds are antiferromagnets with Néel temperatures $T_N\approx300$ K in La_2CuO_4 (Refs. 26 and 27), $T_N\approx500$ K in $YBa_2Cu_3O_6$ (Refs. 26 and 28), and $T_N\approx250$ K in Nd_2CuO_4 (Ref. 29). In the case of p-type doping, the three-dimensional antiferromagnetic ordering is very sensitive to the excess carrier concentration: The long-range magnetic order completely disappears at a concentration of excess holes around 2% (Ref. 44). However, the short-range magnetic order persists at appreciably higher hole concentrations.[45,46] In the case of n-type doping, there is not such a strong effect on the antiferromagnetism of the copper-oxide compounds. The long-range antiferromagnetic order disappears only at a concentration of excess electrons exceeding 14% (Ref. 47). The experiment indicates that in the case of n-type doping a transition to the paramagnetic phase takes place immediately, without intermediate states of spin-glass type.[47]

To obtain a quantitative characterization of the degree of antiferromagnetic ordering of the copper spins in the CuO_2 plane, we used the quantity

$$S=S_0/n_d, \tag{18}$$

where

$$S_0=N^{-1}\sum_i (n_{i\uparrow}-n_{i\downarrow})\exp(i\mathbf{Q}\cdot\mathbf{R}_i)=n^A-n^B \tag{19}$$

is (up to a coefficient) the magnetic moment of the copper antiferromagnetic sublattice per copper atom. In (19), the summation is over only the copper sites, and $\mathbf{Q}=(\pi/a,\pi/a)$. Normalization by the occupancy n_d of the copper orbitals in (18) is convenient in that it enables us to separate precisely the changes in S_0 as a result of doping that are due precisely to the destruction of the antiferromagnetic correlations and not the change in n_d.

Figure 7 gives the results of the calculations of the dependence $S(n)$. The calculations were made for a CuO_2 sheet (the value of S for all n is essentially independent of n beyond $N=256$). Note that $S\neq1$ holds at $n=1$; this is due to the presence in the system of quantum fluctuations. With increasing concentration of excess holes, $n_h=n-1$, or excess electrons, $n_{el}=1-n$, the value of S decreases monotonically (indicating a weakening of the antiferromagnetic correlations) and vanishes at the critical values $n_h^c = n_{el}^c = 0.578$. The phase with $S=0$ is paramagnetic ($n^A=n^B$).

In the case of weak p-type doping, $S(1)-S(n)\approx n-1=n_h$. This can be explained by the formation of Zhang—Rice singlets,[48] the number of which is approximately equal to n_h for $n_h\ll1$. At small values of n_{el}, n-type doping does not have such a strong effect on S as
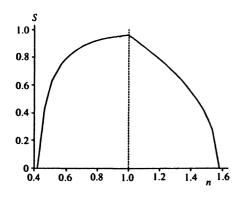
FIG. 9. Dependence of $S(\pi,\pi)$ on ε in the $Cu_{16}O_{32}$ cluster for $U_d/t=6$, $U_p=V=0$, $n=1$. The solid line gives the results of our calculations and the dashed line the data of the Monte Carlo method.[15]

p-type doping. The reason for this is that in the case of n-type doping the excess electrons preferentially occupy copper orbitals[33] (i.e., the value of n_p changes weakly), and therefore, in contrast to the case of p-type doping, no competing interaction that weakens the antiferromagnetic exchange interaction between the spins at the copper sites arises. The small decrease of S at low excess electron concentrations can evidently be attributed to the growth of the effective hopping integral due to the appearance of copper sites not occupied by holes,[49] the number of which is approximately n_{el}. When a certain concentration of excess electrons is reached, S decreases abruptly with a subsequent transition to the paramagnetic phase.

As follows from what has been said above, S depends asymmetrically on n_h and n_{el} in the case of weak doping because the original undoped system with $n=1$ ($n_h=0$, $n_{el}=0$) is a charge-transfer insulator, i.e., has a band gap because of the density of states the nonvanishing value of ε, which in high-T_c superconductors is nevertheless appreciably less than U_d ($\varepsilon/t=1-2$, $U_d/t=6-10$, see Refs. 5 and 7). In the opposite case ($U_d<\varepsilon+2V$), we should have a Mott–Hubbard insulator,[8] and the dependence of S on n_h and n_{el} would be symmetric in the complete range $0\leqslant n_h$, $n_{el}\leqslant 1$ by virtue of the electron–hole symmetry of the Hubbard model. Nevertheless, it is interesting to note that the critical values of n_h^c and n_{el}^c at which S vanishes are equal. Since we consider a purely two-dimensional model, the values of n_h^c and n_{el}^c differ from the corresponding critical values for three-dimensional layer systems [≈ 0.02 (Ref. 44) and ≈ 0.14 (Ref. 47), respectively]. At the same time, the values
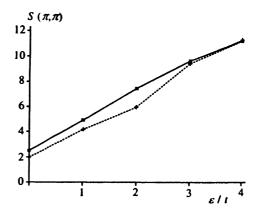
found for n_h^c and n_{el}^c agree well with the results of Ref. 21, in which a two-dimensional model was also used to calculate the dependence of the local magnetic moment at a copper site on the carrier concentration.

In order to compare our data with the results obtained for finite Cu–O clusters by the exact diagonalization method[13] and the Monte Carlo method,[13,15] we calculated

$$m_z^2=N^{-1}\sum_i (S_i^z)^2,$$

$$S(\pi,\pi)=N^{-1}\sum_{i,j} S_i^z S_j^z \exp(i\mathbf{Q}(\mathbf{R}_i-\mathbf{R}_j)),$$

where $S_i^z=n_{i\uparrow}-n_{i\downarrow}$ is twice the total projection of the spin at the i-th copper site [up to a factor, m_z^2 is the mean square of the magnetic moment at the copper sites, and $S(\pi,\pi)$ is the Fourier transform of the spin correlation function, the value of which indicates the strength of the antiferromagnetic correlations of the spins at the copper sites]. The corresponding graphs are given in Figs. 8 and 9 (in each case, the parameters of the Emery model, the temperature, the size of the Cu–O clusters, and the doping levels are the same as in the numerical calculations of Refs. 13 and 15). It can be seen from Figs. 8 and 9 that the agreement between our results and the numerical calculations is fairly good. This is particularly true for the dependence $m_z^2(\varepsilon)$. With regard to the dependence of $S(\pi,\pi)$ on ε, the difference between our data and the results of Ref. 15 reaches 15%. This may be due to
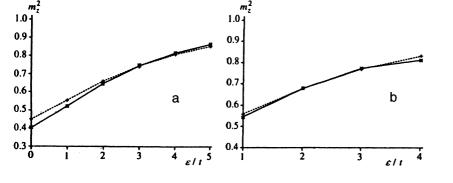
FIG. 8. Dependence of m_z^2 on ε for $U_d/t=6$, $U_p=V=0$, $n=1$. a) The Cu_4O_8 cluster; b) the $Cu_{16}O_{32}$ cluster; the solid lines are the results of our calculations, and the dashed lines are the data of the exact diagonalization method[13] (a) and the Monte Carlo method[15] (b).

the insufficiently high accuracy of the Monte Carlo variational algorithm (used in Ref. 15) compared, for example, with the determinant algorithm (in Fig. 9, the point for $\varepsilon=2$ clearly deviates from a smooth dependence).

6. CONCLUSIONS

In recent years, two broad approaches have developed in the theory of high-T_c superconductors: 1) analytic or semi-analytic treatment of the electronic, magnetic, and superconducting properties of the infinite CuO_2 sheets; 2) exact (or, at least, controllable) numerical calculations made by the Monte Carlo or exact diagonalization methods for finite Cu–O clusters. Each of these approaches has serious shortcomings. The results of the analytic calculations entirely depend on the approximations and simplifications, employed and this often leads not only to quantitative but also to qualitative differences between the data of different authors. On the other hand, exact numerical solutions are possible only for small Cu–O clusters consisting of at most ~ 10 of the CuO_2 unit cells. This is often the reason for lack of confidence in cluster calculations. In this connection, there arises a need for the development of new approaches that, on the one hand, would be to a known extent approximate (and therefore admit almost complete analytic solution) and, on the other, would take into account correctly the interelectron interactions in the CuO_2 sheets. Such methods include, for example, the slave-boson method.[19–21]

In this paper, we have presented a new modified mean-field approximation that satisfies the above requirements: First, it takes into account fairly accurately (in the framework of the Emery model) the presence of antiferromagnetic correlations of the copper spins due to the high energy of the Coulomb repulsion at the copper sites; second, it takes into account other interelectron interactions (at the oxygen sites, between the oxygen and copper sites); third, it admits an almost complete analytic solution and makes it possible to find in explicit form the spectrum of the Fermi quasiparticles (numerical calculations are required only in the self-consistency stage). Comparison with exact numerical calculations for Cu–O clusters showed that the error of our approximation in the calculation of the electronic and magnetic properties (occupancies, magnetic moments, antiferromagnetic correlations) does not, as a rule, exceed 1–5%. The results that we obtained for an infinite CuO_2 sheet agree well with the experimental investigations of the electronic structure of high-T_c superconductors.

Our method has made it possible to estimate the size of a Cu–O cluster above which the electronic properties depend weakly on the number N of CuO_2 cells in the system. We found $N=16$, and this can be regarded as a justification for the use of the exact diagonalization and Monte Carlo methods in the investigation of the electronic structure of the CuO_2 sheets. To study the magnetic properties of doped states, the Cu–O clusters must be somewhat larger, since the characteristic length over which the antiferromagnetic correlations decrease is ~ 3–4 lattice periods (see also Ref. 16).

It is interesting to compare our results with the data of Ref. 50, in which upper and lower bounds on the ground-state energy E_0 were obtained for different carrier concentrations. Our calculations have shown that the values of E_0 satisfy the inequalities $E_0^{min} < E_0 < E_0^{max}$ given in Ref. 50 at least for the parameters of the Emery model that were used in Ref. 50.

Note that the method developed here, in contrast to the slave-boson method, is free of the need to take into account constraints and makes it possible to find the dispersion of the Fermi quasiparticles directly. This facilitates the calculation of the band width, the density of states, and other properties. In addition, the number of parameters that must be determined in the self-consistency stage is smaller in our method than in the slave-boson method. This accelerates the convergence and shortens the time of the numerical calculations by 1–2 orders of magnitude.

We emphasize that our method makes it possible to describe a large number of experimental facts, namely, the nature of the distribution of the carriers between the copper and oxygen sites in the case of p- and n-type doping, the dependence of the Fermi energy on the type of doping and the carrier concentration, the transfer of spectral weight on doping, the more rapid suppression of the antiferromagnetic correlations in the case of p-type doping as compared with n-type doping, etc. All this is achieved for values of the model parameters that correspond to the experiments. The method can be improved further, for example, by taking into account direct oxygen–oxygen hops.

APPENDIX 1

Some relations between the operators $d_{i\sigma}, d_{i\sigma}^A, d_{i\sigma}^B$ are as follows:

1. $d_{i\sigma} = d_{i\sigma}^A + d_{i\sigma}^B$,

$d_{i\sigma}^+ = d_{i\sigma}^{A+} + d_{i\sigma}^{B+}$,

2. $\{d_{i\sigma}^A d_{j\vartheta}^B\} = \{d_{i\sigma}^{A+} d_{j\vartheta}^{B+}\} = \{d_{i\sigma}^{A+} d_{j\vartheta}^B\} = \{d_{i\sigma}^A d_{j\vartheta}^{B+}\} = 0,$

$\{d_{i\sigma}^A d_{j\vartheta}^{A+}\} = 0.5[1 + \sigma \cos(QR_i)]\delta_{ij}\delta_{\sigma\vartheta},$

$\{d_{i\sigma}^B d_{j\vartheta}^{B+}\} = 0.5[1 - \sigma \cos(QR_i)]\delta_{ij}\delta_{\sigma\vartheta},$

where $\{...\}$ is the anticommutator, and δ_{ij} is the Kronecker delta;

3. $n_{i\sigma} = d_{i\sigma}^+ d_{i\sigma} = d_{i\sigma}^{A+} d_{i\sigma}^A + d_{i\sigma}^{B+} d_{i\sigma}^B$.

4. $n_{i\uparrow}n_{i\downarrow} = d_{i\uparrow}^{A+} d_{i\uparrow}^A d_{i\downarrow}^{B+} d_{i\downarrow}^B + d_{i\uparrow}^{A+} d_{i\downarrow}^A d_{i\uparrow}^{B+} d_{i\uparrow}^B$.

APPENDIX 2

The system of equations for the coefficients $C_A, C_B, C_{1A}, C_{1B}, C_{2A}, C_{2B}$ is

$$\begin{cases} (\varepsilon_d^A - E)C_A(\mathbf{k}) - t'X^+ C_{1A}(\mathbf{k}) - t'X^- C_{1B}(\mathbf{k}) - t'Y^+ C_{2A}(\mathbf{k}) - t'Y^- C_{2B}(\mathbf{k}) = 0, \\ (\varepsilon_d^B - E)C_B(\mathbf{k}) - t'X^- C_{1A}(\mathbf{k}) - t'X^+ C_{1B}(\mathbf{k}) - t'Y^- C_{2A}(\mathbf{k}) - t'Y^+ C_{2B}(\mathbf{k}) = 0, \\ -t'X^- C_A(\mathbf{k}) - t'X^+ C_B(\mathbf{k}) + (\varepsilon_p' - E)C_{1A}(\mathbf{k}) = 0, \\ -t'X^+ C_A(\mathbf{k}) - t'X^- C_B(\mathbf{k}) + (\varepsilon_p' - E)C_{1B}(\mathbf{k}) = 0, \\ -t'Y^- C_A(\mathbf{k}) - t'Y^+ C_B(\mathbf{k}) + (\varepsilon_p' - E)C_{2A}(\mathbf{k}) = 0, \\ -t'Y^+ C_A(\mathbf{k}) - t'Y^- C_B(\mathbf{k}) + (\varepsilon_p' - E)C_{2B}(\mathbf{k}) = 0, \end{cases}$$

where

$$X^+ = \exp(ik_x a/2), \quad X^- = \exp(-ik_x a/2),$$

$$Y^+ = \exp(ik_y a/2), \quad Y^- = \exp(-ik_y a/2).$$

APPENDIX 3

The expressions for $E_l(\mathbf{k})$ for $l=3-6$ [the solution of Eq. (12)] are

$$E_3(\mathbf{k}) = -x1 - x2 + x3 + \varepsilon_p' + w/2,$$

$$E_4(\mathbf{k}) = -x1 + x2 - x3 + \varepsilon_p' + w/2,$$

$$E_5(\mathbf{k}) = x1 - x2 - x3 + \varepsilon_p' + w/2,$$

$$E_6(\mathbf{k}) = x1 + x2 + x3 + \varepsilon_p' + w/2,$$

$$w = \varepsilon_d' - \varepsilon_p' + |\varepsilon_d^A - \varepsilon_d^B|/2,$$

$$x1 = \sqrt{2\alpha\sqrt{z}/3 + \beta},$$

$$x2 = \sqrt{\beta - \sqrt{z}[\alpha + \sqrt{3}(1-\alpha^2)]/3},$$

$$x3 = \sqrt{\beta - \sqrt{z}[\alpha - \sqrt{3}(1-\alpha^2)]/3},$$

where

$$\beta = [32t'^2 + (\varepsilon_d^A - \varepsilon_d^B)^2 + 2w^2]/24,$$

$$\alpha = \cos[\cos^{-1}(\gamma/2z^{1.5})/3],$$

$$z = 3t'^4 S(\mathbf{k})(4t'^2 + w^2/4 - (\varepsilon_d^A - \varepsilon_d^B)^2/16)^2$$
$$+ 3t'^2[(\varepsilon_d^A - \varepsilon_d^B)^2 - 16t'^2]/4,$$

$$\gamma = 9t'^4[32t'^2 + (\varepsilon_d^A - \varepsilon_d^B)^2 + 2w^2]S(\mathbf{k})/8$$
$$- [8t'^2 + (\varepsilon_d^A - \varepsilon_d^B)^2/4 - w^2]^3/32 + 9t'^2 w^2[4w^2$$
$$- (\varepsilon_d^A - \varepsilon_d^B)^2 + 16t'^2]/16.$$

APPENDIX 4

The values of $|C_A^l|^2$, $|C_B^l|^2$, $|C_{1A}^l|^2$, $|C_{1B}^l|^2$, $|C_{2A}^l|^2$, $|C_{2B}^l|^2$ for $l=3-6$ are

$$|C_A^l(\mathbf{k})|^2 = [(\varepsilon_p' - E_l(\mathbf{k}))D_l(\mathbf{k})]^2/L_l(\mathbf{k}),$$

$$|C_B^l(\mathbf{k})|^2 = [(\varepsilon_p' - E_l(\mathbf{k}))]^2/L_l(\mathbf{k}),$$

$$|C_{1A}^l(\mathbf{k})|^2 = |C_{1B}^l(\mathbf{k})|^2$$
$$= t'^2[1 + D_l^2(\mathbf{k}) + 2D_l(\mathbf{k})\cos(k_x a)]/L_l(\mathbf{k}),$$

$$|C_{2A}^l(\mathbf{k})|^2 = |C_{2B}^l(\mathbf{k})|^2$$
$$= t'^2[1 + D_l^2(\mathbf{k}) + 2D_l(\mathbf{k})\cos(k_y a)]/L_l(\mathbf{k}),$$

where

$$D_l(\mathbf{k}) = O_l(\mathbf{k})/P_l(\mathbf{k}),$$

$$L_l(\mathbf{k}) = (1 + D_l^2(\mathbf{k}))[(\varepsilon_p' - E_l(\mathbf{k}))^2 + 4t'^2] + 4t'^2 D_l(\mathbf{k})$$
$$\times [\cos(k_x a) + \cos(k_y a)],$$

$$O_l(\mathbf{k}) = (\varepsilon_p' - E_l(\mathbf{k}))(\varepsilon_d^B - E_l(\mathbf{k})) - 4t'^2[\sin^2(k_x a/2)$$
$$+ \sin^2(k_y a/2)],$$

$$P_l(\mathbf{k}) = (\varepsilon_p' - E_l(\mathbf{k}))(\varepsilon_d^A - E_l(\mathbf{k})) - 4t'^2[\sin^2(k_x a/2)$$
$$+ \sin^2(k_y a/2)].$$

We have $|C_A^l(\mathbf{k})|^2 = |C_B^l(\mathbf{k})|^2$ for $U_d = 0$, since $D_l(\mathbf{k}) = 1$ holds by virtue of the fact that $\varepsilon_d^A = \varepsilon_d^B$.

[1] L. F. Mattheiss, Phys. Rev. Lett. **58**, 1028 (1987).
[2] A. Freeman, J. Yu, and C. L. Fu, Phys. Rev. B **36**, 7111 (1987).
[3] J. Ghijsen, L. H. Tjeng, J. van Elp et al., Phys. Rev. B **38**, 11322 (1988).
[4] J. W. Allen, C. G. Olson, M. B. Maple et al., Phys. Rev. Lett. **64**, 595 (1990).
[5] A. K. McMahan, J. F. Annett, and R. M. Martin, Phys. Rev. B **42**, 6268 (1990).
[6] V. J. Emery, Phys. Rev. Lett. **58**, 2794 (1987).
[7] H. Chen and J. Callaway, Phys. Rev. B **40**, 8800 (1989).
[8] J. Zaanen and A. M. Oles, Phys. Rev. B **37**, 9423 (1988).
[9] J. Wagner, A. Muramatsu, and W. Hanke, Phys. Rev. B **42**, 2200 (1990).
[10] V. Hizhnyakov, E. Sigmund, and M. Schneider, Phys. Rev. B **44**, 795 (1991).
[11] J. E. Hirsch, E. Loh, D. J. Scalapino, and S. Tang, Phys. Rev. B **39**, 243 (1989).
[12] V. F. Elesin, V. A. Kashurnikov, L. A. Openov, and A. I. Podlivaev, Zh. Éksp. Teor. Fiz. **99**, 237 (1991) [Sov. Phys. JETP **72**, 133 (1991)]; Zh. Éksp. Teor. Fiz. **101**, 682 (1992) [Sov. Phys. JETP **74**, 363 (1992)].
[13] R. T. Scalettar, D. J. Scalapino, R. L. Sugar, and S. R. White, Phys. Rev. B **44**, 770 (1991).
[14] G. Dopf, A. Muramatsu, and W. Hanke, Physica (Utrecht) C **185–189**, 1495 (1991).
[15] A. Bhattacharya and C. S. Wang, Phys. Rev. B **48**, 13949 (1993).
[16] V. Elesin and V. A. Kashurnikov, Zh. Éksp. Teor. Fiz. **106**, 1773 (1994) [JETP **79**, 961 (1994)].
[17] J. Dutka and A. M. Oles, Phys. Rev. B **42**, 105 (1990).
[18] L. Adamowicz and A. Pondo, Physica (Utrecht) C **192**, 467 (1992).
[19] G. Kotliar and A. Ruckenstein, Phys. Rev. Lett. **57**, 1362 (1986).
[20] W. Zhang, M. Avignon, and K. H. Bennemann, Phys. Rev. B **42**, 10192 (1990).
[21] G. Baumgärtel, J. Schmalian, and K. H. Bennemann, Phys. Rev. B **48**, 3983 (1993); J. Schmalian, G. Baumgärtel, and K.-H. Bennemann, Solid State Commun. **86**, 119 (1993).
[22] A. F. Barabanov, L. A. Maksimov, and G. V. Uĭmin, Zh. Éksp. Teor. Fiz. **96**, 655 (1989) [Sov. Phys. JETP **69**, 371 (1989)].
[23] V. F. Elesin, L. A. Opyonov, E. G. Kholmovskiĭ et al., Pis'ma Zh. Éksp. Teor. Fiz. **61**, 941 (1995) [JETP Lett. **61**, 965 (1995)].

[24] A. F. Barabanov, L. A. Maksimov, and G. V. Uĭmin, Pis'ma Zh. Éksp. Teor. Fiz. **47**, 532 (1988) [JETP Lett. **47**, 622 (1988)].

[25] V. F. Elesin, V. A. Kashurnikov, L. A. Openov, and A. I. Podivaev, Solid State Commun. **89**, 27 (1994).

[26] R. J. Birgeneau and G. Shirane, in *Physical Properties of High Temperature Superconductors*, edited by D. M. Ginsberg (World Scientific, Singapore, 1989).

[27] D. Vaknin, S. K. Sinha, D. E. Moncton *et al.*, Phys. Rev. Lett. **58**, 2802 (1987).

[28] J. M. Tranquada, A. H. Moudden, A. I. Goldman *et al.*, Phys. Rev. B **38**, 2477 (1988).

[29] G. Shirane, in *Proc. of Int. Seminar on HTCS* (Dubna, 1988).

[30] P. Monthoux and D. Pines, Nuovo Cimento D **15**, 181 (1993).

[31] N. Nücker, J. Fink, J. C. Fuggle *et al.*, Phys. Rev. B **37**, 5158 (1988).

[32] Z. Tan, S. M. Heald, S.-W. Cheong *et al.*, Phys. Rev. B **47**, 12365 (1993).

[33] M. Alexander, H. Romberg, N. Nücker *et al.*, Phys. Rev. B **43**, 333 (1991).

[34] S. A. Trugman, Phys. Scr. T **27**, 113 (1989).

[35] J. Wagner, W. Hanke, and D. J. Scalapino, Phys. Rev. B **43**, 10517 (1991).

[36] V. F. Elesin, V. A. Kashurnikov, A. V. Krasheninnikov, and A. I. Podivaev, Physica (Utrecht) C **222**, 127 (1994).

[37] C. T. Chen, F. Settle, Y. Ma *et al.*, Phys. Rev. Lett. **66**, 104 (1991).

[38] H. Romberg, M. Alexander, N. Nücker *et al.*, Phys. Rev. B **42**, 8768 (1990).

[39] S. L. Cooper, G. A. Thomas, J. Orenstein *et al.*, Phys. Rev. B **41**, 11605 (1990).

[40] Y. Tokura, K. Kikuchi, T. Arima, and S. Uchida, Phys. Rev. B **45**, 7580 (1992).

[41] Y. Ohta, T. Tohyama, and S. Maekawa, Phys. Rev. B **66**, 1228 (1991).

[42] R. Liu, W. Vral, A. P. Paulikas *et al.*, Phys. Rev. B **46**, 11056 (1992).

[43] J. M. Allen, Physica (Utrecht) B **171**, 175 (1991).

[44] Y. Endoh, M. Matsuda, K. Yamada *et al.*, Phys. Rev. B **40**, 7023 (1989).

[45] R. J. Birgeneau, D. R. Gabbe, H. P. Jenssen *et al.*, Phys. Rev. B **38**, 6614 (1988).

[46] Yu. A. Izyumov, N. M. Plakida, and Yu. N. Skryabin, Usp. Fiz. Nauk **159**, 621 (1989) [Sov. Phys. Usp. **32**, 1060 (1989)].

[47] G. M. Lüke, L. P. Le, B. J. Sternlieb *et al.*, Phys. Rev. B **42**, 7981 (1990).

[48] F. C. Zhang and T. M. Rice, Phys. Rev. B **37**, 3759 (1988).

[49] W. Zhang and K. H. Bennemann, Phys. Rev. B **45**, 12487 (1992).

[50] T. Wittmann and J. Stolze, Phys. Rev. B **48**, 3479 (1993).

Translated by Julian B. Barbour